

# Ventilation and Low-cost Strategies on Mitigating COVID-19 Infection Disease Transmission in Indoor Environment

Chen Ren<sup>1</sup>, and Shi-Jie Cao<sup>1\*</sup>

<sup>1</sup> Southeast University, School of Architecture, 210096 2 Sipailou Nanjing, China

**Abstract.** During the normalization phase of COVID-19 epidemic, it is gradually reverted to use building space, especially for office. Prevention of airborne pollutant has emerged as a major challenge. Ventilation strategies can mitigate the spread of airborne disease in indoor environment, such as increasing ventilation rate, modifying ventilation mode, etc. The larger ventilation rate can lead to higher energy consumption may not effectively reduce infection risk. The potential of ventilation modes for COVID-19 control should be explored. Furthermore, it is necessary to adopt low-cost strategies, such as physical barrier, to increase the prevention efficiency while combining the ventilation system. This study was to investigate the impact of physical barrier on the spread of particles and infection risk in an office with a sufficient ventilation rate, and then compare different ventilation strategies, including mixing ventilation (MV), zone ventilation (ZV), stratum ventilation (SV) and displacement ventilation (DV), for the optimal one. The simulation model was mainly used in this work and validated by the experiment to show a good agreement with the model prediction. The results showed that (1) the SV showed greater performance in mitigating infection disease spread than MV, ZV and DV, with a minimum infection risk of 13%; (2) a barrier height of at least 60 cm above the desk surface is needed to effectively prevent the transmission of viruses with the risk of infection reduced by about 72%. This work can provide a reference for development of ventilation strategies as well as low-cost prevention interventions in public space oriented the prevention of COVID-19.

## 1 Introduction

Coronavirus disease 2019 (COVID-19) is manifested as a worldwide pandemic, leading to a global issue on the mitigation of severe acute respiratory syndrome coronavirus 2 (SARS-COV-2) [1]. Studies have shown that the aerosol transmission route cannot be ignored, i.e., small-sized droplet nuclei (carrying the virus) from breathing coughing or sneezing become suspended aerosols, further traveling with the air and resulting in human infection [2]. There is growing evidence that SARS-COV-2 has a potential of airborne transmission [3]. The interventions like using physical barrier [4] can be favourable to removal of airborne contaminants, which is dependent on efficient ventilation. In this context, ventilation strategies will play an important role for airborne transmission control especially during the normalization phase of epidemic [5].

Even though physical isolation measures such as wearing mask and keeping social distance are reducing the transmission of aerosol particles, there is still a risk of virus infection in indoor environment. In this sense, proper use of physical barriers can help to decrease the spreading of aerosol particles, thus further reducing the risk of human infection. The critical factors impacting the efficiency of physical barrier include indoor airflow distribution based on different ventilation modes (i.e., location and design of air diffusers).

Ventilation is regarded as a significant strategy to remove contaminant and decreasing the exposure risk, especially in the public spaces such as offices. A study by Li et al. demonstrated that the ventilation rate and airflow pattern are strongly related with the spread of airborne infection disease [6]. However, increasing the ventilation rate will lead to an increase in energy consumption. The design of ventilation modes can help to mitigate the transmission of infection disease and improving the energy saving efficiency. The mixing ventilation (MV) can achieve the dilution of virus by fully mixing with the air. However, at a low supply rate, the mixing effect may yield the problems such as local accumulation of contamination and cross-infection of personnel. To address this issue, the development of different ventilation modes has been a potential, mainly consisting of displacement ventilation (DV), stratum ventilation (SV), zone ventilation (ZV), etc.

This study was to firstly investigate the impact of physical barrier on the infection risk in an office with a sufficient ventilation rate for MV. Then, different ventilation strategies of MV, ZV, SV and DV were compared for the optimal one based on the infection risk. This work can provide a reference for the optimal ventilation strategies and low-cost interventions in a public space oriented the prevention of COVID-19.

## 2 Materials and Methods

\* Corresponding author: [shijie\\_cao@seu.edu.cn](mailto:shijie_cao@seu.edu.cn)

## 2.1 Model setup

The full-scale office model was adopted, with the size of 12.4 m (X) × 9.8 m (Y) × 2.6 m (Z). Figure 1 displays the schematic diagram of various ventilation modes in the office, consisting of MV, ZV, SV and DV. Table 1 illustrates the information of supply air inlets and return air outlets for these ventilation modes. The total area of inlets and outlets was remained the same as 1 m<sup>2</sup> and 0.08 m<sup>2</sup>. The minimum required supply air rate for this office was defined as 1.73 m<sup>3</sup>/s with the percentage of outdoor air of 0.31 and a minimum fresh air of 0.35 m<sup>3</sup>/s [4]. There were totally 43 occupants and 8 rows of desks in this office. The size of desk was set as 0.7 m (X) × 1.2 m (Y) × 0.8 m (Z). The spacing between each row of desks was defined as 1.7 m. The height of physical barrier was designed as 0, 40, 50, 60 and 70 cm above the desk surface.

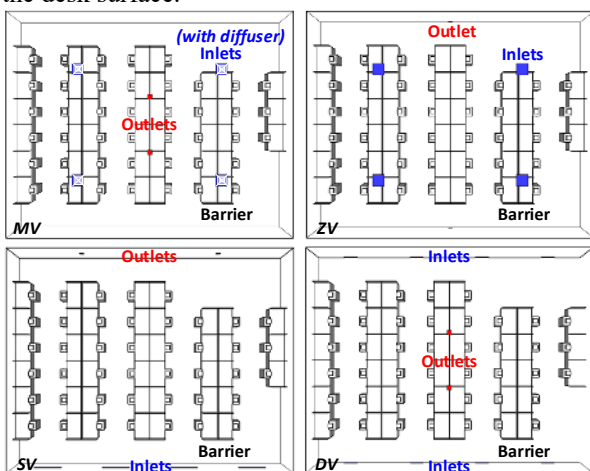


Fig. 1. Schematic diagram of various ventilation modes.

Table 1. Information of different ventilation modes.

Ventilation modes	MV	ZV	SV	DV
inlet size	0.5 m × 0.5 m	0.5 m × 0.5 m	1.25 m × 0.2 m	0.625 m × 0.2 m
outlet size	0.2 m × 0.2 m	0.2 m × 0.2 m	0.2 m × 0.2 m	0.2 m × 0.2 m

In this work, three locations of infected occupant of A, B and C were designed, as shown in Figure 2. The model of occupant was utilized with a body size of 0.4 m (length) × 0.3 m (width) × 1.1 m (height), a head size of 0.2 m (length) × 0.2 m (width) × 0.2 m (height) and a mouth size of 0.02 m (length) × 0.02 m (height). As regards an infected source, the continuous coughing was assumed with the average airflow velocity of 13 m/s downwards at 27.5°. As regards other occupants, the average breathing rate was set to be 0.7 m/s.

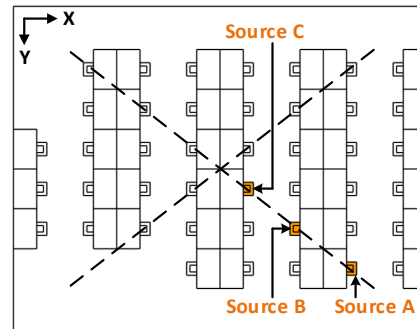


Fig. 2. Layout of three infected occupants in the office.

## 2.2 Experimental study

Testo-405i wireless thermal anemometer was used for measurement of airflow parameters. The measurement accuracy is estimated at ± 0.1m/s with the resolution of 0.01m/s for airflow. The coordinate of measurement point is defined as (x, y) = (4.5 m, 1.55 m), at the alternative heights of 0.4, 0.8, 1.2, 1.6, 2.0 and 2.4 m. For each measurement location, 10 sets of data are obtained within 1 min intervals. In total, 60 groups of measurement samples of airflow rate were acquired.

## 2.3 Numerical simulation

This study utilized computational fluid dynamics (CFD) to simulate the distributions of airflow, air temperature and pollutant concentration. The Reynolds-averaged Navier-Stokes (RANS) equations closed with the renormalization group (RNG) k-ε model were used to predict indoor velocity and temperature fields. The governing equations are shown as below.

$$\nabla \cdot (\rho \bar{u} \varphi) = \nabla \cdot (\Gamma_{\varphi} \nabla \varphi) + S_{\varphi} \quad (1)$$

where,  $\varphi$  is solved variables (velocity and temperature);  $\nabla \cdot (\rho \bar{u} \varphi)$  is convection term;  $\rho$  is air density;  $\bar{u}$  is average airflow velocity;  $\nabla \cdot (\Gamma_{\varphi} \nabla \varphi)$  is diffusion term; and  $S_{\varphi}$  is source term. Next, user-defined scalar (UDS) was adopted to solve the distribution of pollutant by solving the scalar transport equation. It can be assumed to model the aerosols (produced by occupant) carrying virus particles as gaseous pollutants with the influence of pollutant diffusion on indoor airflow neglected. The main reason is that small-sized particles (e.g., aerosols) can follow the air to a longer distance before settling on the surfaces, while large-sized particles will deposit with the distance less than 1 m. The source intensity for infected occupant was assumed as  $1 \times 10^{-4}$  (#/m<sup>3</sup>).

ANSYS Fluent 16.0 was utilized to predict indoor air distribution and pollutant concentration. All the numerical simulations were incompressible and steady-state in this work. The solving can be considered to be converged as the normalized residuals were below  $10^{-4}$  for airflow and air temperature and less than  $10^{-12}$  for UDS. The grid independence analysis between coarse grids (3,417,313), medium grids (8,982,713) and fine grids (13,011,777) was carried out. In this investigation, the grid setup of medium grids was further employed.

The inlets were set as the velocity-inlet, and the supply air temperature was set to be a constant of 25 °C in winter. The outlets were set as the outflow. The wall, physical barrier and desk surface were modeled as non-slip walls. The wall temperature was set to 15 °C. The temperature of occupant body, head and mouth were set as 24 °C, 34 °C and 36 °C, respectively. The airflow temperature for coughing and breathing of occupant was assumed as 36 °C. Table 2 shows an overview of simulation cases in this study.

**Table 2.** Overview of simulation cases.

Case No.	Ventilation mode	Infected source	Barrier height
1-3	MV	A or B or C	0 cm
4-6	MV	A or B or C	40 cm
7-9	MV	A or B or C	50 cm
10-12	MV	A or B or C	60 cm
13-15	MV	A or B or C	70 cm
16-18	ZV	A or B or C	60 cm
19-21	SV	A or B or C	60 cm
22-24	DV	A or B or C	60 cm

## 2.4 Evaluation model

In order to analyze the infection risk under various scenarios of barrier height and ventilation modes, the spatial distribution of pollutant (e.g., virus) predicted by CFD method was used in the Wells-Riley equation. Under the precondition of fully-mixed ventilation, the infection risk can be regarded as a function of exposure time of occupant and pollutant concentration.

$$R_{inf} = \left(1 - e^{-IR^* \int_0^T C(t) dt}\right) * 100\% \quad (2)$$

where,  $R_{inf}$  is infection possibility (%); IR represents the inhalation rate of the exposed occupant ( $m^3/h$ ); T is exposure time (h); and C(t) is pollutant concentration ( $\#/m^3$ ). The inhalation rate of the exposed subjects was considered as the average value of 0.96 ( $m^3/h$ ) between standing and activity states. The exposure time was defined as 1 hour to evaluate the infection possibility in the large open office.

## 3 Results

### 3.1 Validation of simulation and experiment

Figure 3 compares the experimental test and simulation results of airflow and temperature at the location of  $(x, y) = (4.55, 1.55)$  m. It can be found that the average deviation between the results of simulation and field test is 18.5% for velocity and 6.1% for temperature. As regards the grid independence analysis, the simulation results using 8982713 and 13011777 mesh grids can show good agreement, with a deviation less than 5%. Therefore, the grid setup of medium grids was further employed to carry out the simulation.

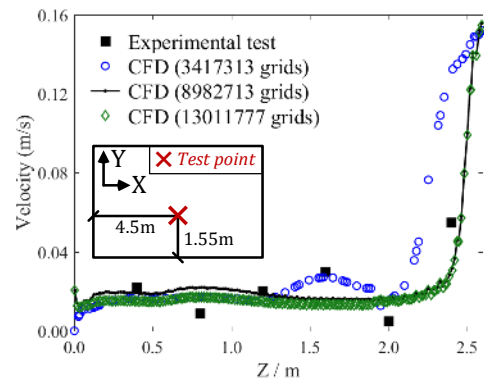


**Fig. 3.** Validations between experimental test and numerical simulation as well as the grid independence analysis.

### 3.2 Influence of barrier height on infection risk

Figure 4 depicts infection risk corresponding to various barrier heights and pollution source locations. Without a physical barrier, the infection risk for a single source of pollution located at point A, B or C positions could be 100%. With implementation of barriers of 40cm and 50 cm, the infection risk can be reduced to 59% and 63%, respectively, for source C. If the barrier height is above 50 cm, infection risk, with a pollutant source at A, can be decreased to 37% and 25%, corresponding to the barrier heights of 60 cm and 70 cm, respectively. In case of a pollution source at B, a barrier height of 60cm can reduce infection risk to about 20%, but infection probability does not significantly decrease with further increase of height. In case of a pollution source at C, infection risk can remain steadily below 10% if barrier height is increased to 60-70 cm. In sense, due to the unknown location of infected personnel in an office, a barrier height of at least 60cm would be appropriate.

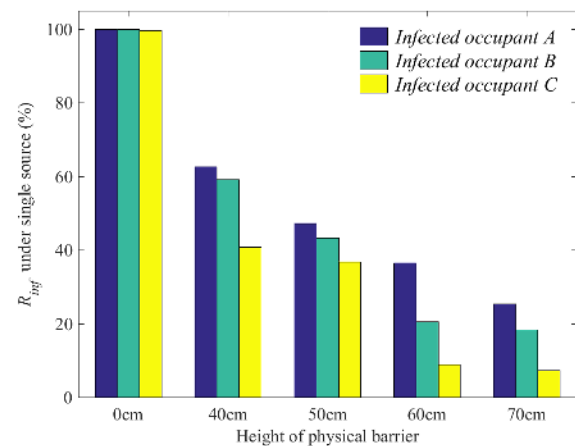


**Fig. 4.** Infection risk (exposure time is 1 hour) for infected source at location A or B or C and barrier heights of 0, 40, 50, 60 and 70 cm.

### 3.3 Influence of ventilation modes on infection risk

Figure 5 depicts the infection risk (with exposure time of 1 hour) corresponding to various ventilation modes of MV, ZV, SV and DV and locations of infected source of A, B, C and A & B & C. For a single infected occupant, the infection risk of occupants under MV and DV

significantly decreased from 37.2% and 33.0% to 9.3% and 8.3%, along with the distance between the infected source and outlet reduced. It further illustrated that the uncertainty of infection risk for MV and DV was resulted in by the layout of outlet. When using MV and DV, it is suggested for occupants to be closer to air outlets. ZV and SV possessed stable performance in diminishing infection risk, with a fluctuation of 4.3% and 9.7% under a single infected source. When the infected source was located at A, the probability of infection for ZV and SV was respectively decreased by 16.9% and 14.5% when compared to that of MV. When the infected source was at the location of B (C), the infection risk under ZV and SV could be increased by 9.2% (6.7%) and 9.7% (3.7%) in comparison to that of MV. Considering the average infection probability under the scenarios of three single infected sources (A or B or C), ZV and SV both contributed to a minimum risk of about 19.4% and DV resulted in a maximum value of about 22.5%.

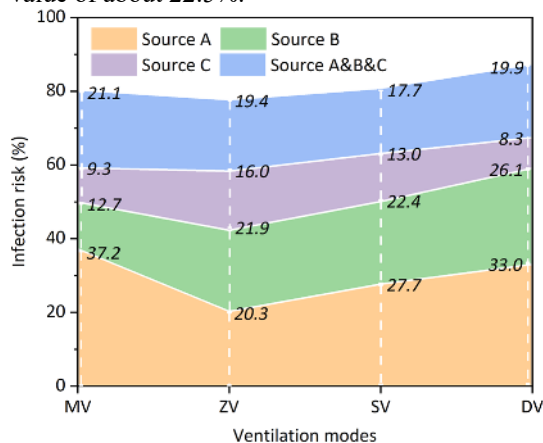


**Fig. 5.** Infection risk (with exposure time of 1 hour) under different ventilation modes and locations of infected source.

## 4 Discussion

The limitations of this study are discussed. Firstly, this work used a simplified rectangular model to represent the occupants in an office to significantly reduce the computational cost. The 3D model with realistic human geometry for occupants should be further considered. Secondly, steady-state simulation was carried out in this study. However, the transmission of virus such as SARS-CoV-2 was associated to unsteady boundary conditions and indoor airflow fields, which should be explored in the future study. Thirdly, in addition to airborne transmission, the droplet transmission mode of COVID-19 can play a significant role in infection of occupants. Future studies should take into account the evaporation process from liquid droplet to droplet nucleus during coughing or sneezing, the deposition of virus particles in indoor environment as well as the transmission risk of droplet, in order to improve the reliability of evaluation of overall infection probability under different ventilation systems.

## 5 Conclusions

This study was to investigate the impact of physical barrier height on the infection risk in an office with a ventilation strategy of MV. Then, different ventilation strategies of MV, ZV, SV and DV were compared for the optimal one based on the results of infection risk. The main conclusions are shown as follows.

In case location and number of infection source is unknown, a barrier height of at least 60cm above the desk is recommended provided a sufficient ventilation rate. SV showed a good performance in mitigating the transmission of airborne infectious disease in an office room. The infection risk in indoor environment using MV and DV was greatly dependent on the distance between infected occupant and air outlets.

## References

1. F. Salamone, B. Barozzi, A. Bellazzi, L. Belussi, L. Danza, A. Devitofrancesco, M. Ghellere, I. Meroni, F. Scamoni, C. Scrosati, *Buildings* **11**, 660 (2021)
2. L. Morawska, J. L. W. Tang, W. Bahnfleth, P. M. Bluyssen, A. Boerstra, G. Buonanno, J. J. Cao, S. Dancer, A. Floto, F. Franchimon. How can airborne transmission of COVID-19 indoors be minimised? *Environ. Int.* **142**, 105832 (2020)
3. J. Y. Wan, J. J. Wei, Y. T. Lin, T. F. Zhang, Numerical Investigation of Bioaerosol Transport in a Compact Lavatory. *Buildings* **11**, 526 (2021)
4. C. Ren, C. Xi, J. Q. Wang, Z. B. Feng, F. Nasiri, S. J. Cao, F. Haghghat, *Sustain. Cities. Soc.* **74**, 103175 (2021)
5. J. W. Ding, C. W. Yu, S. J. Cao, *Indoor Built. Environ.* **29**, 9 (2020)
6. Y. Li, G. M. Leung; J. W. Tang, X. Yang, C. Y. H. Chao, J. Z. Lin, J. W. Lu, P. V. Nielsen, J. Niu, H. Qian, *Indoor Air* **17**, 1 (2007)